Proton Positions in the Mn 2+ Binding Site of Concanavalin A as Determined by Single-Crystal High-Field ENDOR Spectroscopy

ARTICLE *in* JOURNAL OF THE AMERICAN CHEMICAL SOCIETY · SEPTEMBER 2001

Impact Factor: 12.11 · DOI: 10.1021/ja015136r · Source: PubMed

4 AUTHORS, INCLUDING:

Raanan Carmielli
Weizmann Institute of Science
44 PUBLICATIONS **866** CITATIONS

SEE PROFILE

Proton Positions in the Mn^{2+} Binding Site of Concanavalin A as Determined by Single-Crystal High-Field ENDOR Spectroscopy

Raanan Carmieli,[†] Palanichamy Manikandan,[†] A. Joseph Kalb (Gilboa),[‡] and Daniella Goldfarb*,[†]

Contribution from the Departments of Chemical Physics and Structural Biology, The Weizmann Institute of Science, Rehovot, Israel 76100

Received February 19, 2001. Revised Manuscript Received May 16, 2001

Abstract: High-field (95 GHz) pulsed EPR and electron−nuclear double resonance (ENDOR) techniques have been used for the first time to determine coordinates of ligand protons of a high-spin metal center in a protein single crystal. The protein concanavalin A contains a Mn^{2+} ion which is coordinated to two water molecules, a histidine residue, and three carboxylates. Single crystals of concanavalin A were grown in H_2O and in D_2O to distinguish the exchangeable water protons from the nonexchangeable protons of the imidazole group. Distinct EPR transitions were selected by performing the ENDOR measurements at different magnetic fields within the EPR spectrum. This selection, combined with the large thermal polarization achieved at 4.5 K and a magnetic field of ∼3.4 T allowed us to assign the ENDOR signals to their respective M_S manifolds, thus providing the signs of the hyperfine couplings. Rotation patterns were acquired in the *ac* and *ab* crystallographic planes. Two distinct crystallographic sites were identified in each plane, and the hyperfine tensors of two of the imidazole protons and the four water protons were determined by simulations of the rotation patterns. All protons have axially symmetric hyperfine tensors and, by applying the point−dipole approximation, the positions of the various protons relative to the Mn^{2+} ion were determined. Likewise, the water protons involved in H-bonding to neighboring residues were identified using the published, ultrahigh-resolution X-ray crystallographic coordinates of the protein (Deacon et al. *J. Chem. Soc., Faraday Trans.* **1997**, *93*(24), 4305−4312).

Introduction

X-ray crystallography is by far the most established and effective method for determining the three-dimensional (3D) structure of proteins. One limitation of this technique is the difficulty in determining proton positions. This is particularly problematic in the case of H_2O and OH^- which cannot be distinguished.[1,2] Moreover, the orientation of the OH bond(s) with respect to other protein residues cannot be determined as long as the proton positions are unknown. The latter are of significance as they reveal the presence of hydrogen bonds which are very important in structure stabilization and in reactions involving proton transfer. In metalloproteins or metalloenzymes water molecules or OH^- anions often serve as ligands to the metal ion. The detailed characterization of the metal site requires the identification of all of its ligands, particularly when they differ in their structural and electronic characteristics that determine the properties of the site. In addition, the position and orientation of H_2O and OH^- ligands may be significant in terms of the function of the site. When the metal center is paramagnetic, electron−nuclear double resonance (ENDOR) measurements on single crystals can provide the missing information on the exact location of the protons.[3−6]

ENDOR spectroscopy has been applied extensively in the past to study metal ion sites in frozen solutions of metalloproteins and metalloenzymes. Such studies have led to the identification of ligands and to the determination of distances between the metal and the magnetic nuclei.[7−9] In many instances, when orientation-selective ENDOR measurements are possible, the orientation of the ligand with respect to the local symmetry axis, given by the *g*-tensor, may be determined as well.[10] Precise atomic coordinates, however, can only be obtained from single-crystal measurements.[3−6] Protein single crystals are frequently too small to provide adequate signal intensities for ENDOR measurements at conventional X-band frequencies (9 GHz). Consequently, the recent developments in high-field EPR and ENDOR spectroscopy offer unique opportunities to overcome this sensitivity problem. This has been demonstrated by the pioneering work of Coremanes et al.,[11,12] where the complete hyperfine and quadrupole tensors of weakly

[†] Departments of Chemical Physics.

[‡] Departments of Chemical Physics and Structural Biology.

(1) Thomann, H.; Bernardo, M.; Kroneck, P. M. H.; Ulrich, V.; Goldfarb, D. *J. Am. Chem. Soc.* **1995**, *117*, 8243−8251.

(2) Goldfarb, D.; Thomann, H.; Bernardo, M.; Kroneck, P. M. H.; Ulrich, V. *J. Am. Chem. Soc.* **1996**, *118*, 2686−2693.

(3) Metz, H.; Kuechler, J.; Bötcher, R. *Chem. Phys. Lett.* **1982**, *89*, 352−354.

(4) Metz, H.; Kuechler, J.; Bötcher, R. *Chem. Phys. Lett.* **1983**, *97*, 303−307.

(5) Bötcher, R.; Heinhold, D.; Windsch, W. *Chem. Phys. Lett.* **1979**, *65*, 452−455.

(6) Metz, H.; Bötcher, R.; Windsch, W. *Chem. Phys. Lett.* **1986**, *127*, 278−282.

(7) Hüttermann, J. In *Biological Magnetic Resonance*; Berliner, L. J., Reuben, J., Eds.; Plenum Press, New York, 1993; Vol. 13, pp 219−253.

(8) Hoffmann, B. M.; Derose, V. J.; Doan, P. E.; Gubriel, R. J.; Houseman, A.; Tesler, J. In *Biological Magnetic Resonance*; Berliner, L. J., Reuben, J., Eds.; Plenum Press, New York, 1993; Vol. 13, pp 151−218.

(9) Thomann, H.; Bernardo, M. In *Biological Magnetic Resonance*; Berliner, L. J., Reuben, J., Eds.; Plenum Press, New York, 1993; Vol. 13, pp 275−322.

(10) Hurst, G. C.; Henderson, T. A.; Kreilick, R. W. *J. Am. Chem. Soc.* **1985**, *107*, 7294−7299.

(11) Coremans, J. W. A.; Poluektov, O. G.; Groenen, E. J. J.; Canters, G. W.; Nar, H.; Messerschmidt, A. *J. Am. Chem. Soc.* **1994**, *116*, 3097−3101.

10.1021/ja0104305 CCC: $20.00
Published on Web 08/02/2001

coupled ^{14}N nuclei in the Cu(II) site in single crystals of azurin were determined.

For half-integer, high spin systems, such as Mn^{2+} (d^5, $S = {}^5/_2$), high-field EPR/ENDOR offers, besides increased sensitivity, additional important advantages. For a system with a dominating electron Zeeman interaction and a significant zero-field splitting (ZFS), the intensities of the forbidden transitions are considerably reduced, thus increasing the spectral resolution.[13] Furthermore, the large thermal polarization that can be achieved at low temperatures allows for a straightforward assignment of the ENDOR lines to their respective electron-spin manifolds, M_S, thus providing the sign of the hyperfine coupling.[14,15] In this work we report on detailed single-crystal W-band (95 GHz) ^1H ENDOR measurements on the Mn^{2+} site of the protein concanavalin A. From these measurements we have determined the positions of the protons of water and imidazole ligands. To the best of our knowledge, this is the first example of a protein single-crystal ENDOR study of a high-spin center in which proton coordinates have been determined.

Concanavalin A is a member of the plant hemagglutinin (or plant lectin) family; a large and ubiquitous group of saccharide-binding proteins whose biological function is as yet unknown.[16] The importance of these proteins is expressed in their ability to bind saccharides; each member of the family has a unique saccharide specificity.[16] The 3D structure of concanavalin A has been recently determined at an exceptionally high resolution, 0.94 Å.[17] The overall structure of the stable protein dimer is dominated by an extensive β sheet strand arrangement, the so-called jellyroll motif. This further associates as a dimer of dimers to form a tetramer of 100 kDa total molecular weight. Each monomer has a molecular weight of 25 kDa comprising 237 amino acids and containing two metal binding sites. One, called S1, is occupied by a transition metal ion, for example, Mn^{2+}, and the other, S2, by Ca^{2+}. Occupancy of both sites is essential for saccharide binding. The Mn^{2+} site has a slightly distorted octahedral geometry in which the Mn^{2+} is coordinated to the carboxyl groups of asp10, asp19, and glu8, the imidazole N_ϵ of his24, and two water molecules. The carboxyl groups of asp10 and asp19 form a bridge to the Ca^{2+}. The role of the transition metal in this protein is structural: the Mn^{2+}, together with the Ca^{2+}, serve as stabilizers for the loops that constitute the saccharide binding site. The crystal has an orthorhombic symmetry (space group I_{222}), with unit cell parameters $a = 89.2$ Å, $b = 87.2$ Å, $c = 62.9$ Å. The ZFS of the Mn^{2+} ion has been determined by single-crystal Q-band continuous wave (CW) EPR spectroscopy.[18]

Recently, we have reported a W-band ENDOR investigation of the hyperfine coupling of the imidazole and water protons in the Mn^{2+} site of conacanavalin A in a frozen solution.[14] In that study the principal components of the hyperfine tensors of the protons were determined, and the strategy of signal assignment in high spin systems under large thermal polarization was established. In the present work we applied this strategy to single crystals where the Mn−H distances obtained earlier from the frozen solution results have been refined, and the orientation of the hyperfine tensors with respect to the crystallographic axes have been determined. This allowed us to calculate the atomic coordinates of the protons and to substantiate the presence of hydrogen bonds with neighboring residues.

Experimental Section

Sample Preparation and Crystal Growth. A lyophilized powder of concanavalin A was purchased from Pharmacia. The crystallization buffer (XTAL) was prepared by mixing 0.05 M Tris buffer with 0.1 M $NaNO_3$ (or 0.4 M $NaNO_3$ for D_2O XTAL), adjusting the pH to 6.5 with acetic acid, and adding 1 mM $CdSO_4$ and 1 mM $CaCl_2$.[19] Concanavalin A powder, 100 mg, was dissolved in 4 mL of saturated NaCl solution and then gently shaken at 313 K for 2 h. The sample was then centrifuged briefly at room temperature to remove small amounts of undissolved material and passed through a Millipore filter of 0.22 μm pore size. Dialysis bags containing 0.2 mL of the protein solution were immersed in vials containing XTAL buffer and were incubated at 303 K for several days, until sizable crystals of well-shaped morphology appeared in the dialysis tubes. This procedure produced well-shaped crystals where the long axis of the crystal, which is the HOL bisector, is parallel to the crystallographic *b* axis, the *c* axis is perpendicular to [001], and *a* is parallel to [001].

The crystals chosen for the ENDOR measurements ($\sim 0.7 \times 0.4 \times 0.3$ mm^3 and $\sim 0.4 \times 0.4 \times 0.3$ mm^3 for measurements in the *ac* and *ab* planes, respectively) were transferred into a XTAL/MPD (2-methyl-2,4-pentanediol) (50:50%) solution where the MPD serves as a cryoprotectant. MPD, with deuterated hydroxyl groups, was prepared by three cycles of distillation and D_2O addition to normal MPD. The crystals were mounted, with the aid of a polarizing microscope, into 0.9-mm-o.d. thin-walled quartz tubes with their crystallographic *b*- or c axes parallel to the long axis of the tube. The excess of liquid was carefully removed with the help of a wet filter paper, until the crystal was barely wet, and the tube was carefully flame-sealed at both ends. The exact orientation of the crystal was determined by brief X-ray diffraction measurements using a Nonius Kappa CCD diffractometer and MoKα radiation. Prior to the low-temperature EPR/ENDOR measurements, the crystals were flash-frozen by immersion in liquid nitrogen for a few seconds and then immediately inserted into the precooled spectrometer.

Spectroscopic Measurements. All spectroscopic measurements were carried out at 4.4−4.6 K on a home-built spectrometer operating at 94.9 GHz.[20] Field-sweep echo-detected (FS-ED) EPR spectra were recorded using the two-pulse echo sequence ($^\pi/_2 - \tau - \pi - \tau - echo$) where the echo intensity is measured as a function of the magnetic field. Typically, microwave (MW) pulse lengths (t_{MW}) of 0.05 and 0.1 μs were used with $\tau = 0.25$ μs. The magnetic field values were calibrated using the proton Larmor frequency, as determined by the ENDOR measurements. ^1H ENDOR spectra were measured using the Davies ENDOR pulse sequence ($\pi - T - {}^\pi/_2 - \tau - \pi - \tau - echo$, with a RF pulse applied during the time interval *T*).[21] The Mims ENDOR sequence ($^\pi/_2 - \tau - {}^\pi/_2 - T - {}^\pi/_2 - \tau - echo$, with a RF pulse applied during the time *T*) was used for the ^2H ENDOR measurements.[22] The experimental conditions were: $t_{MW} = 0.2$, 0.1, 0.2 μs, $\tau = 0.4$ μs, $t_{RF} = 25$ μs in the Davies ENDOR experiments, and $t_{MW} = 0.1$, 0.1, 0.1 μs, $\tau = 0.25$ μs, $t_{RF} = 40$ μs for the Mims ENDOR measurements. Relatively long RF pulses had to be used to avoid broadening of the narrow ^1H signals. The intensity and frequency scales of the ^2H ENDOR spectra were multiplied by -1 and γ^H/γ^D

(12) Coremans, J. W. A.; Poluektov, O. G.; Groenen, E. J. J.; Canters, G. W.; Nar, H.; Messerschmidt, A. *J. Am. Chem. Soc.* **1996**, *118*, 12141−12153.

(13) Arieli, D.; Vaughan, D. E. W.; Strohmaier, K. G.; Goldfarb, D. *J. Am. Chem. Soc.* **1999**, *121*, 6028−6032.

(14) Manikandan, P.; Carmieli, R.; Shane, T.; Kalb (Gilboa), A. J.; Goldfarb, D. *J. Am. Chem. Soc.* **2000**, *122*, 3488−3494.

(15) Goldfarb, D.; Strohmaier, K. G.; Vaughan, D. E. W.; Thomann, H.; Poluektov, O. G.; Schmidt, J. *J. Am. Chem. Soc.* **1996**, *118*, 4665−4671.

(16) Kalb (Gilboa), A. J.; Habash, J.; Hunter, N. S.; H. J. Price, H. J.; J. Raftery, J.; J. R. Helliwell, J. R. *Metal Ions in Biological Systems*; M. Dekker, Inc.: New York, 2000; Vol. 37, pp 279−304.

(17) Deacon, A. T.; Gleichmann, T.; Kalb (Gilboa), A. J.; Price, H. J.; Raftery, J.; Brabbrook, G.; Yariv, J.; Helliwell, J. R. *J. Chem. Soc., Faraday Trans.* **1997**, *93(24)*, 4305−4312.

(18) Meirovitch, E.; Luz, Z.; Kalb, A. J. *J. Am. Chem. Soc.* **1974a**, *96*, 7538−7541.

(19) Greer, J.; Kaufman, H. W.; Kalb, A. J. *J. Mol. Biol.* **1970**, *48*, 365−366.

(20) Gromov, I.; Krymov, V.; Manikandan, P.; Arieli, D.; Goldfarb, D. *J. Magn. Reson.* **1999**, *139*, 8−17.

(21) Davies, E. R. *Phys. Lett.* **1974**, *47A*, 1−2.

(22) Mims, W. B. *Proc. R. Soc.* **1965**, *283A*, 452−457.

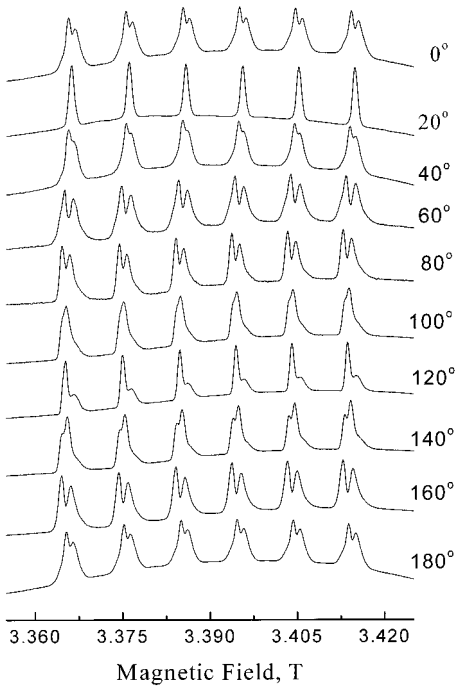

Figure 1. Angular dependent W-band FS-ED EPR spectra of a concanavalin A single crystal in the *ac* plane. The rotation angles are noted on the figure.

Table 1. Euler Angles Relating the Principal Axis System of the Hyperfine Tensor with the Crystallographic Axis System for the Four Different Mn^{2+} Sites of Conacanavalin A

site I	α	β	γ
site II	α	β	$\gamma + 180$
site III	α	$180 - \beta$	$180 - \gamma$
site IV	α	$180 - \beta$	$-\gamma$

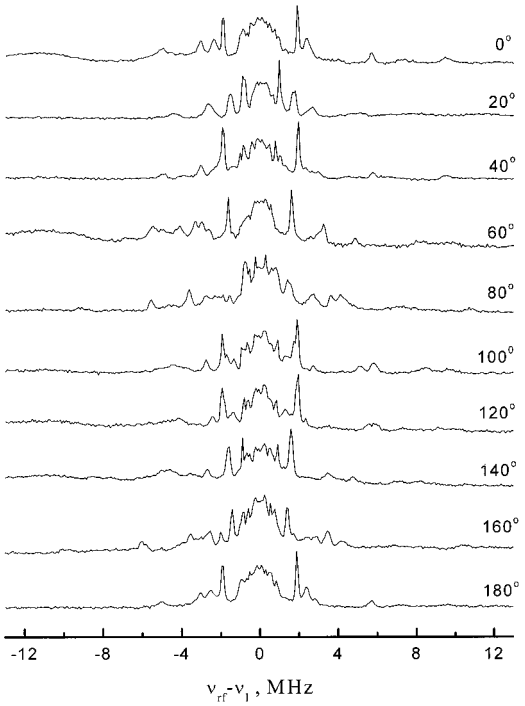

Figure 2. ^{1}H ENDOR spectra in the *ac* plane of a concanavalin A single-crystal grown in H_2O. The rotation angles are noted on the figure.

(=6.5144), respectively, to allow convenient comparison with the ^{1}H ENDOR spectra. The frequency scale in the ^{1}H and ^{2}H ENDOR spectra is given with respect to the Larmor frequency, $\nu = \nu_{RF} - \nu_I$.

Simulations and Data Analysis. The ENDOR frequencies of a $S = 5/2$ system coupled to a $I = 1/2$ nucleus are given by:[23]

$$\nu_{M_S}^{ENDOR} = [(M_S A - \nu_I)^2 + M_S{}^2 B^2]^{12} \quad (1)$$

where ν_I is the Larmor frequency, $A = T_\perp(3\cos^2\theta - 1) + a_{iso}$ and $B = 3\,T_\perp \sin\theta\cos\theta$. a_{iso} is the isotropic hyperfine constant, and θ is the angle between the direction of the unique axis of the hyperfine interaction and the external magnetic field, $\vec{B}$. Equation 1 is valid for a axially symmetric hyperfine interaction and, when the point−dipole approximation applies, $T_\perp$ is related to the electron−nuclear distance r according to:

$$T_\perp = \frac{g g_N \beta \beta_N}{h r^3} \quad (2)$$

and the unique axis of the interaction is along $\vec{r}$. Equation 1 applies for a system with a dominating electron Zeeman interaction and relatively small ZFS and isotropic hyperfine coupling, so that the ENDOR frequencies are not affected by the ZFS.[24] Moreover, at high fields the B dependent term in eq 1 can be neglected.

When $I = 1$, there are two ENDOR transitions for each M_S manifold, given to first order by:[8,25]

$$\nu_{M_S}^{ENDOR}(\pm) = \nu_{M_S}^{ENDOR} \pm \frac{3}{2}P \quad (3)$$

where P is the angular-dependent nuclear quadrupole splitting.

The frequency separation of the various EPR transitions is significantly larger than the MW pulse bandwidth even for samples with small ZFS. Therefore, for each paramagnetic center only one EPR transition is selected during a pulse experiment. However, due to the inhomogeneous broadening of the EPR spectrum, the selection of a particular magnetic field results in the excitation of a number of overlapping EPR transitions arising from different centers. At ~3.3 T ($g \simeq 2$) and low temperatures, the EPR energy levels are highly polarized, and the contributions of the $|^1/_2, m\rangle \rightarrow |^3/_2, m\rangle$ and $|^3/_2, m\rangle \rightarrow |^5/_2, m\rangle$ EPR transitions to the ENDOR spectrum are relatively small. Consequently, the ENDOR spectrum should exhibit primarily signals from the $M_S = -^5/_2, -^3/_2, -^1/_2, ^1/_2$ manifolds.

The ^{1}H ENDOR single-crystal rotation patterns of the $M_S = \pm^1/_2$ manifolds were simulated using a program based on eq 1, and the best fit was done using the E04FYF routine of NAG. For convenience, the following reference frames were used: the principal axis system of the hyperfine interaction $P(x,y,z)$, the crystal frame $C(c,b,a)$, the sample tube frame $T(x',y',z')$, where z' is parallel to the tube axis, the goniometer frame $G(x'',y'',z'')$, and the lab frame $B(X,Y,Z)$, where $Z \parallel \vec{B}$. The transformation between these axes systems is described via the appropriate Euler angles, and the hyperfine tensor transformations are carried out using the corresponding Wigner rotation matrixes, $R(\alpha',\beta',\gamma')$. For our experimental setup the transformations are:

$$P \xrightarrow{0,\beta,\gamma} C \xrightarrow{\phi,\theta,\psi} T \xrightarrow{0,0,\phi_0} G \xrightarrow{\phi_r,90,0} B \quad (4)$$

The rotation patterns were acquired by measuring the spectrum as a function of the rotation angle of the goniometer, ϕ_r. The relation between the above sets of angles and the angle θ in eq 1 is given by:

$$R(0,\theta,0) = R(0,\beta,\gamma)\,R(\phi,\theta,\psi)\,R(0,0,\phi_0)\,R(\phi_r,90,0) \quad (5)$$

There are four Mn^{2+} centers per unit cell in the crystals of concanavalin A and, according to the symmetry properties of the I_{222} space group, their orientations are related as described in Table 1. The values of a_{iso}, $T_\perp$, β, and γ for each proton were obtained from best fit

(23) Kurreck, H.; Kirste, B.; Lubitz, W. *Electron Nuclear Double Resonance Spectroscopy of Radicals in Solution Application to Organic and Biological Chemistry*; VCH Publishers: New York, 1988.

(24) Vardi, R.; Bernardo, M.; Thomman H.; Strohmaier, K. G.; Vaughan, D. E. W.; Goldfrab, D. *J. Magn. Reson.* **1997**, *126*, 229−241.

(25) Gemperle, C.; Schweiger, A. *Chem Rev.* **1991**, *91*, 1481−1505.

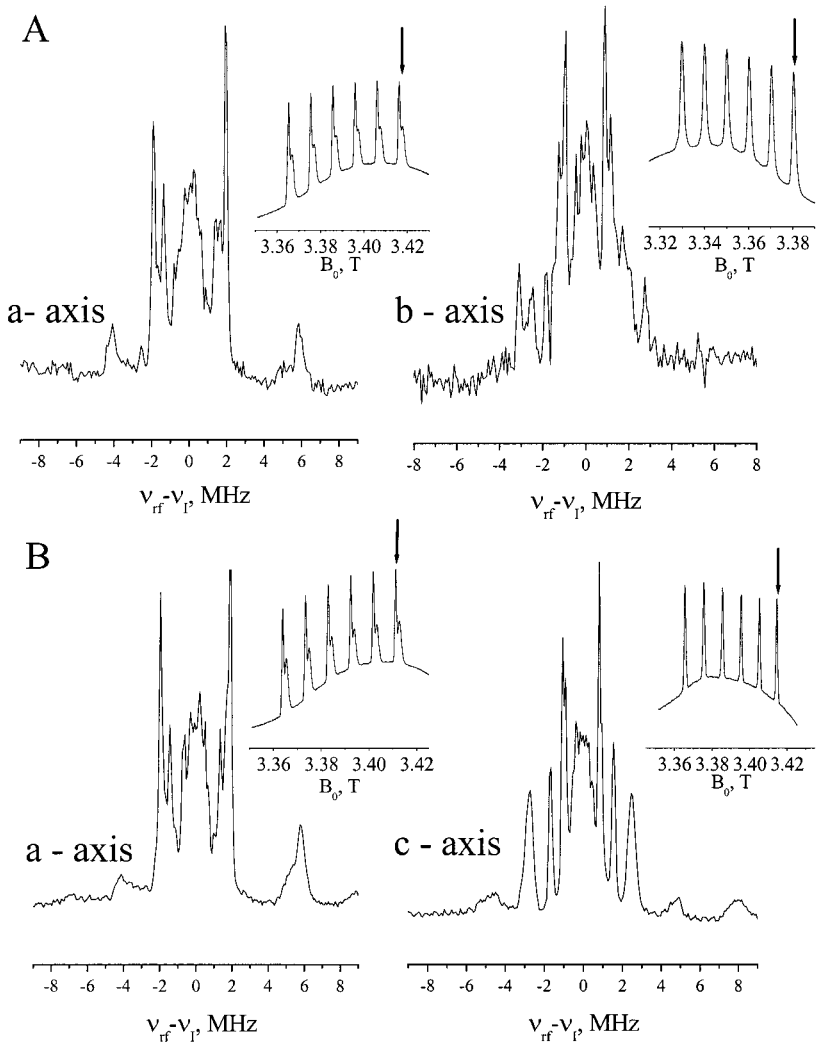

Figure 3. ^{1}H ENDOR spectra of a concanavalin A single-crystal recorded with $\vec{B}$ along the crystallographic axes in the *ab* (A) and *ac* (B) planes. The insets show the corresponding FS-ED EPR spectrum, and the arrows indicate the field where the ENDOR spectra were recorded.

simulations of the ENDOR rotation patterns of the $M_S = \pm^1/_2$ manifolds. All angles in eq 4, besides β and γ are defined by the experimental conditions. In this work we have measured rotation patterns only in two crystallographic planes, *ab* and *ac*. This is sufficient for a unique determination of the above parameters because we know from our earlier study on the frozen solution that the water and imidazole protons have an axial hyperfine interaction.[14,26] Moreover, the sign of the hyperfine splitting at each orientation can be determined due to the large thermal polarization achieved at high fields and low temperatures.[14,26]

Results

A single crystal of concanavalin A with a regular morphology was oriented with its *b* axis parallel to the sample tube axis (perpendicular to the direction of the external magnetic field). FS-ED EPR spectra, recorded as a function of the orientation of the magnetic field, ϕ_r, in the crytallographic *ac* plane, are shown in Figure 1. The region shown corresponds to the well-resolved ^{55}Mn hyperfine sextet of the $|-^1/_2, m\rangle \rightarrow |^1/_2, m\rangle$ EPR transitions. The signals due to the other EPR transitions appear as a broad background with some angular dependence and unresolved ^{55}Mn hyperfine splitting. The low resolution of these transitions has been attributed to a mosaic spread of ZFS parameters.[18] The spectra exhibit two well-resolved sets of sharp sextets of the spectroscopically distinct Mn^{2+} sites in this plane. At $\phi_r = 20°$ the sextets of the two sites merge, indicating that the magnetic field is along one of the crystallographic axes. At this orientation, the weak forbidden transitions, ($\Delta m_S = \pm 1$, $\Delta m_I = \pm 1$) situated between the sextet lines, become evident.

For each crystal orientation, ^{1}H ENDOR spectra were acquired at the magnetic field corresponding to the highest field ^{55}Mn hyperfine component. This line is often split due to the presence of distinct crystallographic sites (see Figure 1), and ENDOR spectra were recorded for each site. Figure 2 shows the angular dependence of the ENDOR spectrum in the *ac* plane, where only the spectrum corresponding to the most intense feature of the composite EPR line is displayed. A second crystal was oriented with its *c* axis parallel to the tube axis and FS-ED EPR spectra and ENDOR spectra were recorded with the magnetic field in the *ab* plane (spectra not shown).

The identification of the EPR spectra corresponding to a particular crystallographic axis was done using the ENDOR spectra. Since the rotation patterns were acquired in two

(26) Here we show using a simple geometrical model that the two planes provide all of the information needed. In the case of an axially symmetric hyperfine tensor, a rotation pattern of 180° about any of the crystallographic axes will cross once the plane at which the splitting corresponds to $A_\perp$, and at this this point the splitting will correspond to a minimum in the pattern. Identifying this point in the two planes provides (1) $A_\perp = a_{iso} - T_\perp$. Then, from the hyperfine splitting measured when the field is along each of the crystallographic axes we obtain (2) $A_c = a_{iso} + T_\perp (3 \sin^2 \beta \cos^2 \gamma - 1)$, (3) $A_b = a_{iso} + T_\perp (3 \sin^2 \beta \sin^2 \gamma - 1)$, (4) $A_c = a_{iso} + T_\perp (3 \cos^2 \beta - 1)$. Since we also know the signs of all the splittings, we have four independent equations for determining four parameters.

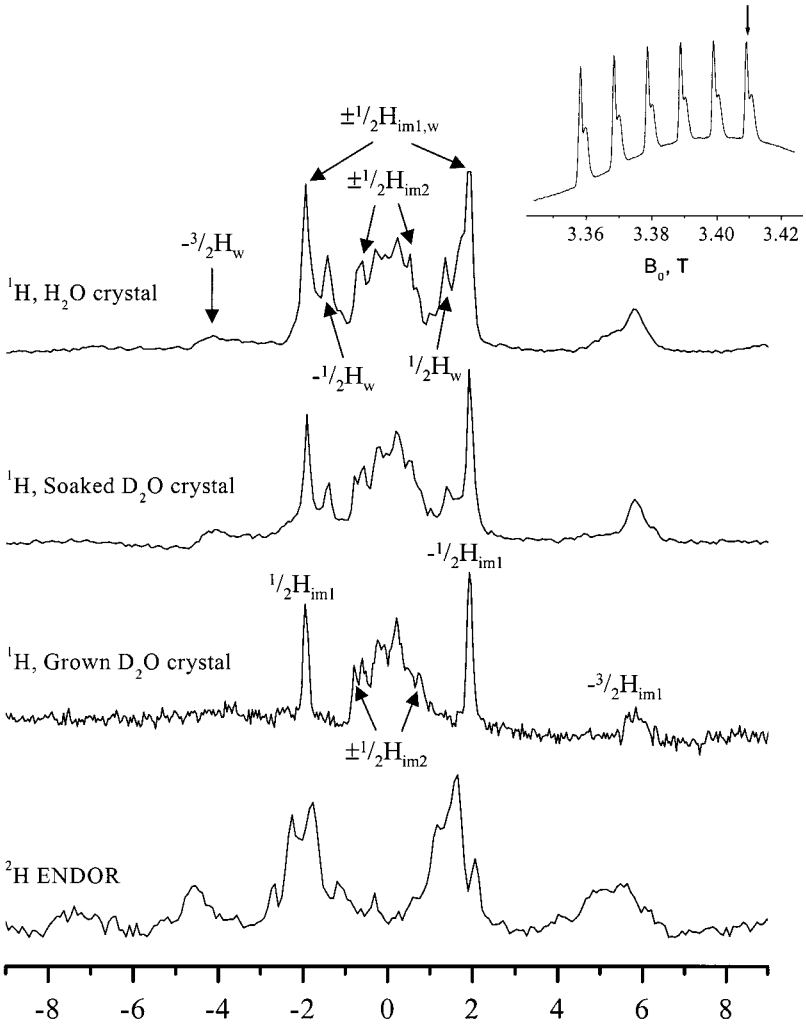

Figure 4. ^{1}H and ^{2}H ENDOR spectra of concanavalin A single crystals, as noted on the figure, with the magnetic field along the crystallographic *a* axis, $B_0 = 3.4126$ *T*. The signals marked with H_w and H_{im} indicate water and imidazole protons, respectively. In addition, the signals are labeled according to their respective manifolds.

crytallographic planes, *ab* and *ac*, the situation when the magnetic field is along *a* occurs in both planes. Therefore, the ENDOR spectra recorded along this axis in the two planes should be identical. Figure 3 shows the ^{1}H ENDOR and FS-ED EPR spectra recorded with the magnetic field parallel to the crystallographic axes in the *ac* and *ab* planes. The ENDOR spectra on the left-hand side are similar for both planes, thus assigning this orientation to the *a* axis. The spectra on the right-hand side correspond to the other two crystallographic axes.

The FS-ED EPR spectrum of a crystal with I_{222} symmetry, recorded at $a \parallel \vec{B}$ should exhibit a single sextet since all four Mn^{2+} sites become magnetically equivalent, as is observed for $c \parallel \vec{B}$ and $b \parallel \vec{B}$. In contrast, a shoulder appears next to each of the sextet lines, indicating that the four Mn^{2+} ions are not magnetically equivalent. The possibility that these extra signals arise from a misalignment of the crystal is ruled out since we have checked the crystal alignment at room temperature using X-ray diffraction and we have verified that the freezing procedure does not alter the crystal orientation. Moreover, the same spectrum was reproduced from many different crystals with the same alignment. We therefore ascribe this splitting to a temperature-induced change in the local symmetry relation between the four Mn^{2+} sites to which the ZFS is most sensitive. This transition requires extensive investigation and will not be discussed here any further.

The ^{1}H ENDOR spectra consist of signals of water and imidazole protons which overlap at certain orientations. The assignment of the signals was done by comparison of the ^{1}H ENDOR spectra in the *ac* plane with those of a crystal grown in D_2O. Figure 4 illustrates the strategy for signal assignment. Initially, we used crystals that were soaked in D_2O, but the exchange was found to be incomplete. The partial exchange is attributed to slow diffusion of the D_2O molecules in the crystal. In contrast, growing the crystals in D_2O and using deuterated MPD resulted in complete disappearance of the water signals from the ^{1}H ENDOR spectrum as shown in Figure 4 (bottom trace). At this particular crystal orientation the spectrum consists of symmetric doublets, corresponding to the $M_S = \pm^1/_2$ manifolds of the imidazole protons, H_{im1} and H_{im2}, that appear at ± 1.94 and ± 0.7 MHz, respectively. The line at 5.85 MHz is due to the H_{im1} signal of the $M_S = -3/2$. The ^{2}H ENDOR spectrum was recorded to verify the assignment of the signals of the water protons. Indeed, the bottom spectrum in Figure 4 shows that the ^{2}H peaks appear at the expected positions. This procedure was carried out for all orientations, allowing us to the determine the individual rotation patterns of H_{im1} and H_{im2}. A complete rotation pattern of a crystal grown in D_2O was recorded only for the *ac* plane. This was sufficient because once the rotation patterns of the imidazole protons in this plane were identified, it was possible to assign the spectra in the *ab* plane

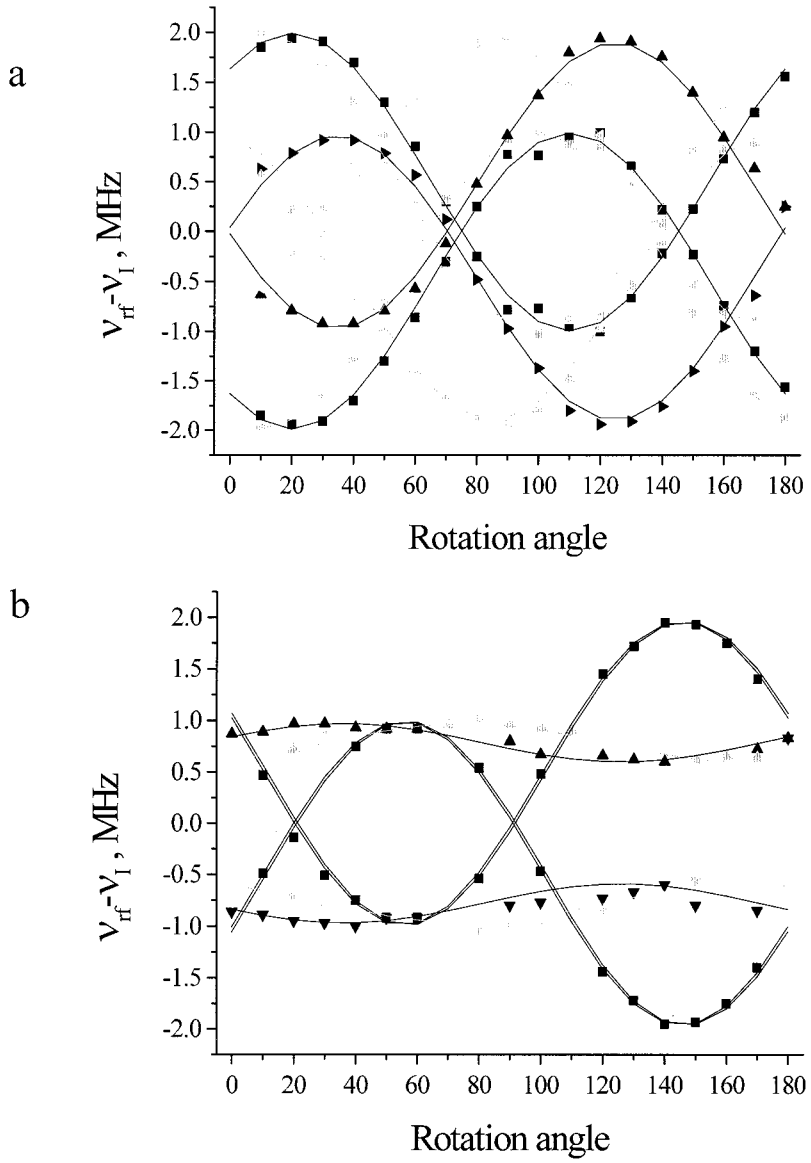

Figure 5. (a) ^{1}H ENDOR rotation patterns of the imidazole protons in the (a) *ac* and (b) *ab* planes. The square and the triangles indicate H_{im2} and H_{im1}, respectively, and the gray and black marks indicate sites I and II, respectively.

by using the spectrum recorded along *a*. All ENDOR spectra show a number of lines with very small couplings that are due to remote protons. These have not been assigned and will not be discussed further.

Finally, the signs of the hyperfine splittings were determined by assigning the ENDOR signals to their respective $M_S = \pm^1/_2$ manifolds. This was achieved by recording the ENDOR spectra at magnetic field positions where the contributions of the $|-^1/_2, m\rangle \rightarrow |^1/_2, m\rangle$ transitions are negligible and those of the $|-^3/_2, m\rangle \rightarrow |-^1/_2, m\rangle$ are substantial.[14] In such spectra the contribution of the $M_S = {}^1/_2$ ENDOR line is considerably diminished.

Analysis of the Imidazole Protons. The ^{1}H ENDOR rotation patterns of the $M_S = \pm^1/_2$ imidazole protons in the *ac* and *ab* planes are shown in Figure 5. Initially, only doublets with relatively large couplings in one plane that were easy to identify and assign were taken into account, and the final fitting procedure was done by fitting simultaneously the rotation patterns of the two planes. The assignment of doublets with splittings below ±0.7 MHz is difficult because of overlap with distant protons. Moreover, the Davies ENDOR experiment is not sensitive to small coupling, and therefore their intensities are diminished. The assignment of these data points was completed using the simulated rotation patterns. The *ac* rotation pattern (Figure 5a) shows that two distinct sites are present and their spectra coincide at $\phi_r = 15°$ ($a \,||\, \vec{B}$) and $\phi_r = 105°$ ($c \,||\, \vec{B}$). Similarly, in the *ab*, plane two sites can be easily distinguished for one of the protons, and they coincide at rotation angles of 59° and 149°, where $\vec{B} \,||\, b$ and $\vec{B} \,||\, a$, respectively. The rotation patterns in Figure 5b show that for one of the protons the Mn−H vector is perpendicular to the *ab* plane since it is almost

Table 2. Summary of the Hyperfine Coupling Constants of the Imidazole and Water Protons[a]

proton	$T_\perp$, (± 0.04) MHz	a_{iso}, (± 0.04) MHz	β ± 0.5 (deg)	γ ± 0.5 (deg)	r_{Mn-H} ± 0.02 Å
H_{im1}	1.94	0.08	83	−70.3	3.44
H_{im2}	1.99	0.08	89.5	5.3	3.41
H_{w1}	3.49	0.8	78.3 (83.1)	143.0 (142.4)	2.82 (2.77)
H_{w2}	3.96	0.1	112.9 (110.6)	134.0 (154.8)	2.71 (3.08)
H_{w3}	2.5	0.4	47.0 (56.2)	50.0 (47.2)	3.16 (2.87)
H_{w4}	3.9	0.4	67.0 (58.2)	72.0 (84.8)	2.72 (2.63)

[a] The numbers in parentheses were calculated from neutron diffraction data.[28]

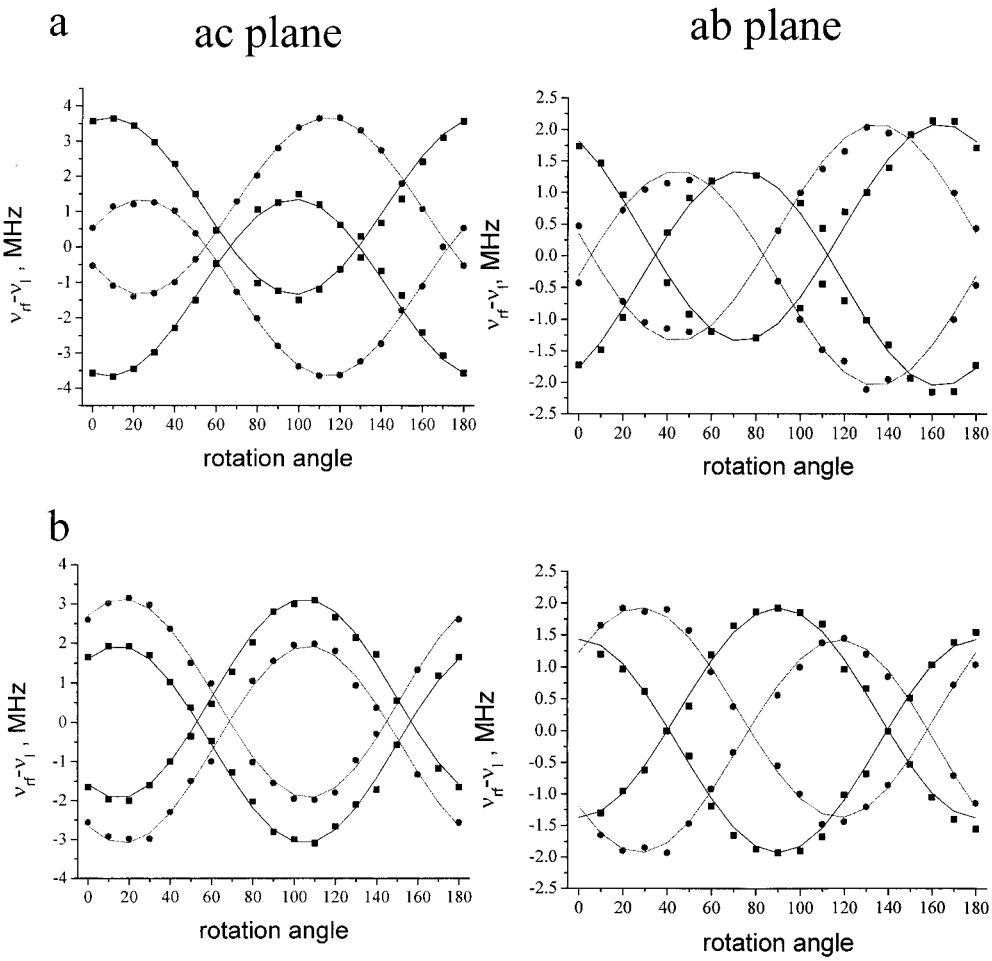

Figure 6. ^{1}H ENDOR rotation patterns of the (a) H_{w1} and (b) H_{w2} water protons in the *ac* and *ab* plane. The squares and the circles indicate sites I and II, respectively.

impossible to distinguish between the two sites. Unlike the ZFS, the ENDOR data behave as expected for I_{222} symmetry; the signals of the different crystallographic sites merge when the magnetic field is parallel to any of the crystallographic axes. The hyperfine tensor parameters of the two imidazole protons obtained from the fit of the rotation patterns are listed in Table 2. From the rotation patterns we obtained four different sets of parameters for each proton. Those belonging to one molecule (listed in Table 1) were identified by taking into account the imidazole group geometry as a constraint, namely, H−H distances were calculated from the Mn−H distances and orientations. The parameters of the other three centers can be obtained by the relation given in Table 1.

Analysis of the Water Protons. Once the signals of the imidazole protons were assigned, it was possible to extract the rotation patterns of the water protons and analyze them by following the same strategy outlined for the imidazole protons. Four different protons were identified, and the rotation patterns of H_{w1} and H_{w2}, and H_{w3} and H_{w4} in the *ac* and *ab* planes are presented in Figures 6 and 7, respectively. Each of these rotation patterns show that two different sites can be identified in each crystallographic plane. Similar to the imidazole protons, the sites become equivalent when $\vec{B}$ is along the axes, as expected for I_{222} symmetry. The best fit simulated rotation patterns for each proton are presented as solid lines in Figures 6 and 7 and the a_{iso}, $T_\perp$, β, and γ values obtained are listed in Table 2. The Mn−H distances were determined using the point−dipole approximation (see eq 2). All distances determined in this work are larger than 2.7 Å. These relatively long distances, along with the small a_{iso} values obtained for all protons support the validity of the point-dipole approximation in our case, as also applied for $Mn(H_2O)_6^{2+}$ by Tan et al.[27] From the rotation patterns, we obtained four different sets of parameters for each proton. Those belonging to one molecule were identified as described for the imidazole protons where the water molecule geometry was taken into account, namely calculating H−H distances. All of the parameters listed in Table 2 are consistent with all protons belonging to one Mn^{2+} center, where H_{w1} and H_{w2} belong to one water molecule and H_{w3} and H_{w4} to the second water molecule. The parameters of the other three centers can be obtained by the relations given in Table 1.

Discussion

The single-crystal measurements, due to their higher resolution, revealed that there are small differences between the Mn−H distances of the imidazole protons compared to the results obtained in our earlier work on a frozen solution (3.56 ± 0.04 Å) of concanavalin A.[14] The values obtained, $T_\perp(H_{im1}) = 1.94 \pm 0.04$ MHz, and $T_\perp(H_{im2}) = 1.99 \pm 0.04$ MHz, correspond to distances of 3.44 ± 0.02 and 3.41 ± 0.02 Å, respectively. On the basis of the proton coordinates we obtained and by using the X-ray coordinates of the imidazole group,[17] H_{im1} is assigned to H_δ and H_{im2} to H_ϵ (see Figure 5). The proton positions determined from the ENDOR measurement are in very good agreement with the 3D structure where the protons were

(27) Tan, X.; Bernardo, M.; Thomann, H.; Scholes, C. P. *J. Chem. Phys.* **1993**, *98*, 5147−5157.

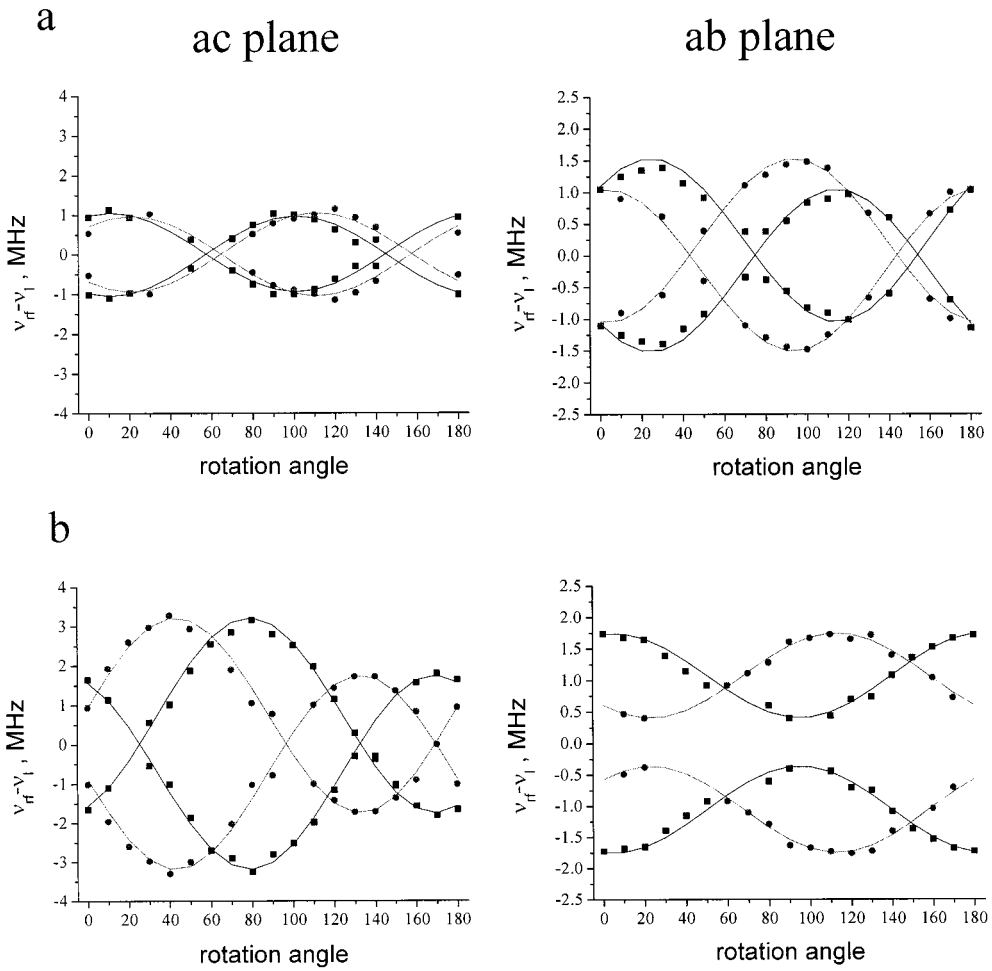

Figure 7. ^{1}H ENDOR rotation patterns of the (a) H_{w3} and (b) H_{w4} water protons in the *ac* and *ab* plane. The squares and the circles indicate sites I and II, respectively.

added using the molecular modeling software of Insight II. This structure gives $\beta = 83°$, $\gamma = -70.1°$ and $\beta = 89.5°$, $\gamma = 5.3°$ and the distances are 3.41 and 3.49 Å for H_ϵ and for H_δ respectively. These compare very well with the values determined from the ENDOR measurements (see Table 2). The hyperfine tensors of the imidazole protons can be used in the future as a reference to identify imidazole ligands in Mn^{2+} sites in proteins of unknown structures.

The earlier frozen solution study[14] also provided estimates for the Mn−H distances and a_{iso} values of the water protons. The distances obtained were 2.67 ± 0.04, 2.76 ± 0.04, 2.99 ± 0.04, and 3.24 ± 0.04 Å which compare favorably with 2.71 ± 0.02, 2.72 ± 0.02, 2.82 ± 0.02, and 3.16 ± 0.02 Å. The values of a_{iso} show some disagreement; the frozen solution values are 0.03 ± 0.08, 0.86 ± 0.08, 0.08 ± 0.08, and 0.21 ± 0.08 MHz compared to 0.1 ± 0.04, 0.4 ± 0.04, 0.8 ± 0.04, and 0.4 ± 0.04 MHz obtained from the present work. We attribute the discrepancy between the frozen solution and the single-crystal results to the experimental error in $A_\parallel$ and $A_\perp$ arising from the overlapping powder patterns of the various protons and to the uncertainty in a_{iso} originating from ambiguity in finding the $A_\parallel$ and $A_\perp$ pairs.[14]

Using the hyperfine tensor parameters summarized in Table 2, we calculated the coordinates of the water and imidazole protons and added them to the crystal structure[17] as shown in Figure 8. The assignment of the protons to the two different water oxygens, O_{412} and O_{413}, of the crystal structure was done by calculation the O−H distance using the ENDOR and X-ray determined coordinates. This gave $O_{412}-H_{w1}$ and $O_{412}-H_{w2}$ distances of 1.16 and 0.97 Å, respectively, and a $HO_{412}H$ angle of 104.6°. The distance between H_{w1} and H_{w2} is 1.69 Å. In the second water molecule, the $H_{w3}-H_{w4}$ distance is 1.46 Å, and the $O_{413}-H_{w3}$ and $O_{413}-H_{w4}$ distances are 1.1 and 1.05 Å, respectively. The calculated HO_{413} H angle, however, is 86°, which is too small. Nevertheless, if O_{413} is moved 0.05 Å away from the Mn^{2+} ion, the angle increases to 102.3°. An error of 0.05 Å in the oxygen position cannot be excluded, considering the X-ray diffraction resolution. Our results show that both water ligands are ordered in the crystal, at least at low temperatures. The proton coordinates show that they are involved in hydrogen bonds, thus besides acting as ligands, the water molecules also have a role in stabilizing the tertiary structure of the protein. In Table 3 we list the distances of the various protons from nearby oxygens. H_{w1} and H_{w2} are hydrogen-bonded to Val32 and Glu8, whereas H_{w3} and H_{w4} are close to the oxygen (O_γ) of the hydroxyl group of Ser34. However, since it is unlikely that the latter is involved in two H-bonds, the existence of $O-H_{w4}-(O_\gamma)$Ser34 seems more likely due to the shorter distance and larger angle.

Recently, neutron diffraction measurements on D_2O grown crystals of concanavalin A were carried out at room temperature at a resolution of 2.4 Å to determine the coordinates of bound water molecules.[28] Out of the four deuterons of the Mn^{2+} water ligands, three were detected. The fourth, one of the O_{413} water molecules, could not be observed, and its position was determined by modeling. Using the neutron diffraction-determined

(28) Habash, J.; Raftery, J.; Nuttall, R.; Price, H. J.; Wilkinson, C.; Kalb (Gilboa), A. J.; Helliwell, J. R. *Acta Crystallogr.* **2000**, *D56*, 541−550.

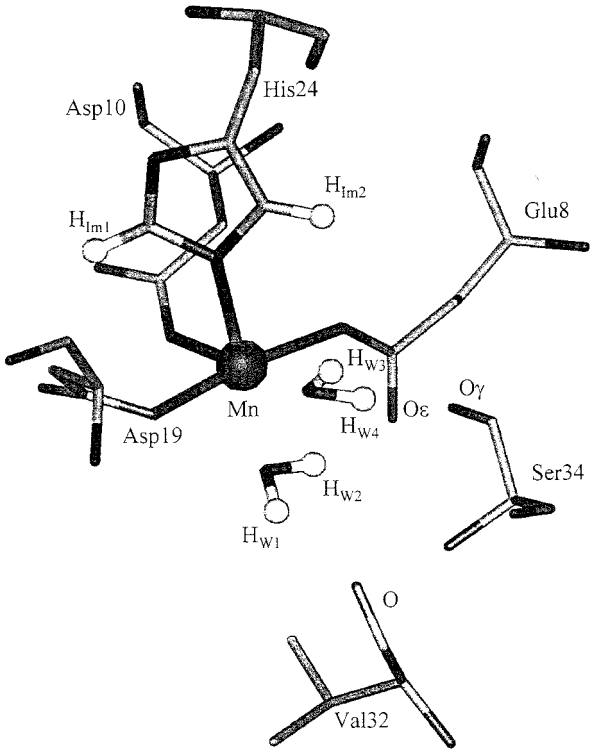

Figure 8. Binding site of the Mn^{2+} ion in concanavalin A.[17] The protons were added according to the coordinates determined from this work.

deuteron coordinates, we have calculated $T_\perp$ and the orientation of the Mn−H vectors with respect to the crystallographic axes (see Table 2, values are listed in parentheses). Then, using these values we tried to fit our experimental rotation patterns leaving only a_{iso} of each water proton as a free parameter. The agreement between the calculated and the experimental patterns was not satisfactory. The major discrepancies between the ENDOR results and the neutron diffraction results are in the Mn−H distances of H_{w1} and H_{w3}. For comparison, we also list in Table 3 the D-bonding distances and D−O−D angles obtained from the neutron diffraction data. We attribute the discrepancies to the relatively low resolution of the neutron diffraction results (see, for example, neutron density maps of the waters linked to the Mn^{2+} Figure 4, ref 28). In addition, the measurement temperature should also be taken into account. At room temperature some mobility of the water ligands is expected, and the measurements provide the average position with a large temperature factor. In contrast, at low temperature the motion is frozen, and the water molecules assume their lower-energy position.

Table 3. Hydrogen-Bonding Network of the Two Water Molecules, Taking the Proton Coordinates from the ENDOR Results and the Residue Coordinates from the X-ray Determined Crystal Structure[17] [a]

donor	acceptor	H - - O (Å)	O−H - - O (deg)
H_{w1}	Val32 O	2.03 (2.1)	132.4 (141.9)
H_{w2}	Glu8 $O_{\epsilon 2}$	1.77 (2.65)	156.3 (79.3)
H_{w4}	Ser34 O_γ	1.62 Å(2.14)	166.8 (117.6)

[a] The values in parentheses correspond to the neutron diffraction data.[28]

Conclusions

W-band pulsed ENDOR experiments were performed on single crystals of the protein concanavalin A. Using a selection of different EPR transitions and D_2O exchange, an assignment strategy was established. The coordinates of the H_δ and H_ϵ imidazole protons, and of the protons of two water molecules ligands were determined. The two imidazole protons are nearly magnetically equivalent, and their hyperfine coupling is purely dipolar. The water molecules were found to be ordered and involved in H-bonding with Glu8, Ser34, and Val32.

This work demonstrates for the first time "ENDOR crystallography for protons" for high-spin metal sites in proteins. Several properties of high-field EPR/ENDOR spectroscopy made such experiments plausible: (i) high sensitivity that allows measurements on small protein crystals, (ii) high resolution of the Mn^{2+} ion EPR spectrum due to the reduced intensity of the forbidden transitions, (iii) relatively high frequency of ^2H ENDOR signals which facilitates their detection, and finally (iv) large thermal polarization that allows the assignment of the various ENDOR peaks to their specific M_S manifolds. In principle, such experiments should also be plausible for $S = {}^1/_2$ systems in proteins.

Acknowledgment. This research was supported by the DFG Schwerpunkt program "High field EPR in Physics, Chemistry and Biology", the Israel Science Foundation, administered by the Israeli Academy of Sciences and Humanities. We thank Dr. Linda Shimon for her help with the determination of crystal orientation by X-ray diffraction. We thank Dr. B. Epel and Professor Z. Luz for many helpful discussions.

JA0104305